IAOx induces the SUR phenotype and differential signalling from IAA under different types of nitrogen nutrition in *Medicago truncatula* roots

Javier Buezo[a], Raquel Esteban[b, c], Alfonso Cornejo[d], Pedro López-Gómez[a], Daniel Marino[c], Alejandro Chamizo-Ampudia[a], María J. Gil[d], Víctor Martínez-Merino[d], Jose F. Moran[a]

[a]*Department of Sciences-Institute of Multidisciplinary Applied Biology Research-IMAB, Public University of Navarre; Avenida de Pamplona 123; 31192 Mutilva, Spain*

[b]*Basque Centre for climate Change (BC3), 48640 Leioa, Spain*

[c]*University of the Basque Country, UPV/EHU; Sarriena s/n; Apdo. 644; 48080 Bilbao, Spain*

[d]*Department of Sciences-Institute for Advance Materials INAMAT , Public University of Navarre; Campus de Arrosadia; 31006 Pamplona, Spain*

Abstract

Indole-3-acetaldoxime (IAOx) is a particularly relevant molecule as an intermediate in the pathway for tryptophan-dependent auxin biosynthesis. The role of IAOx in growth-signalling and root phenotype is poorly studied in cruciferous plants and mostly unknown in non-cruciferous plants. We synthesized IAOx and applied it to *M. truncatula* plants grown axenically with NO_3^-, NH_4^+ or urea as the sole nitrogen source. During 14 days of growth, we demonstrated that IAOx induced an increase in the number of lateral roots, especially under NH_4^+ nutrition, while elongation of the main root was inhibited. This phenotype is similar to the phenotype known as "superroot" previously described in SUR1- and SUR2-defective *Arabidopsis* mutants. The effect of IAOx, IAA or the combination of both on the root phenotype was different and dependent on the type of N-nutrition. Our results also showed the endogenous importance of IAOx in a legume plant in relation to IAA metabolism, and suggested IAOx long-distance transport depending on the nitrogen source provided. Finally, our results point out to CYP71A as the major responsible enzymes for IAA synthesis from IAOx.

Authors for correspondence:

Jose Fernando Moran

jose.moran@unavarra.es

Tlf: +34 948168018

Keywords: Ammonium, auxin, indole-3-acetaldoxime, nitrate, oximes, phenotype, superroot, root, urea, CYP71A.

Abbreviations: Aldehyde oxidase, AO; Cytochrome P450 family 71A, CYP71A; IAA oxidase, IAA-*Ox*; Indole-3-acetaldehyde, IAAld; Indole-3-acetaldoxime, IAOx; Indole-3-acetic acid, IAA; Indole-3-acetonitrile, IAN; Indole-3-pyruvic acid, IPyA; Nitric oxide, NO; Polar auxin transport inhibitor sensitive1, PIS1; SUPERROOT1, SUR1; SUPERROOT2, SUR2; superroot index, SRI; Seedlings grown with IAOx, $_{OX}$nutrition; Tryptophan, Trp

Funding

This work was supported by the grants AGL2017-86293-P, CGL2017-84723-P (IBERYCA) and AGL2014-52396-P, from the Spanish Ministry of Economy and Competitiveness (MINECO) and the Ministry of Science Innovation and Universities (MICINN) and by the Basque Government (IT932-16). JB and PL-G are holders of PhD fellowships from the Public University of Navarre. ACh received a Juan de la Cierva initiation grant FJCI-2016-27905 and RE received a Juan de la Cierva incorporation grant IJCI-2014-21452. This research was also supported by the Basque Government through the BERC 2018-2021 program, and by the Spanish Ministry of Science, Innovation and Universities through the BC3 María de Maeztu excellence accreditation (MDM-2017-0714).

1. Introduction

Indole-3-acetaldoxyme (IAOx) is produced after the N-hydroxylation and subsequent decarboxylation of tryptophan (Trp). IAOx is a particularly relevant molecule that has been proposed as a precursor of indole-3-acetic acid (IAA) in a major biosynthetic pathway [1,2]. In *Arabidopsis thaliana*, IAOx is produced from the CYP79B pathway by the cytochrome P450 monooxygenases, CYP79B2 and CYP79B3 [3]. The Trp-dependent IAA biosynthesis pathway through IAOx has been widely studied in the *Brassicaceae* family, especially in *A. thaliana* [4], however, the mechanisms whereby IAA is produced from IAOx are still unclear. Nevertheless, increases in both IAOx and IAA levels have been reported recently in *Zea mays* in response to herbivory [5]. Although the Trp-dependent IAA synthesis route has been thoroughly studied [6], the details of the entire pathway are still a matter of debate as the implicated genes and associated enzymes seem to be redundant, and the active IAA-level is efficiently regulated by the plant [6]. Thus, different pathways referring to IAOx have been described by different authors [6–8]. IAOx can be dehydrated to IAN by an IAOx dehydratase (CYP71A13 in *A. thaliana*) [6] or transformed to indole acetaldehyde (IAAld). Both routes can subsequently produce IAA, either by a nitrilase or by an indole-acetaldehyde oxidase (AO) [7].

Besides being an IAA precursor, in Brassicaceae IAOx is also an intermediate in the biosynthesis of compounds such as glucosinolates or camalexin [2]. The IAOx conversion to glucosinolates requires, among other enzymes, SUPERROOT1 (SUR1) and SUPERROOT2 (SUR2) [9]. The loss-of-function mutants *sur1* and *sur2* of *A. thaliana* showed a massive number of adventitious roots and a high-auxin behaviour phenotype, which is also known as the "superroot" phenotype [9,10]. Indeed, previous works have proposed that disruption of the glucosinolate pathway leads to IAOx accumulation, subsequently enhancing IAA production, and thus results in this phenotype [2, 4]. On the other hand, the effects of IAA in plant development and other diverse biological mechanisms have been well described (reviewed in ref [11,12])

It is known that auxins, including IAA, can be transported into the cell by the Polar Auxin Transport Inhibitor Sensitive1 (PIS1) transporter, which belongs to the ABCG37 transporter family. These transporters have been shown to transport indole-3-butyric acid and they may well transport other similar compounds [13]. Conversely, NO_3^- transporters regulate auxin biosynthesis genes. Indeed, the NRT1.1 transporter and NO_3^- itself participate in the regulation of endogenous auxin uptake in root cells [14]. Besides, auxins are known for stimulating lateral root development, although the signalling mechanism is not fully understood

yet. On the other side, and in contrast to NO_3^- , supplying NH_4^+ or urea as the only N source usually represents a stress condition for a great variety of plant species[15]

IAOx is essential for plant growth and abiotic stress responses [16]. Indeed, several studies suggest that IAOx in Brassicaceae may be an important metabolic switch between production of IAA and glucosinolates, optimizing fitness in a changing environment [2,3,17]. However, the biological importance of IAOx and its role in signalling under different N sources remains unclear. Even though IAOx seems to be biologically active, its role in plant developmental signalling is still unknown. In this work, we applied different doses of synthesized IAOx to assess the interplay between IAOx and different N sources (NO_3^-, NH_4^+ and urea) during the development of *M. truncatula* roots according to their phenotypical and biochemical characteristics.

2. Materials and methods

2.1. Reagents, chemical synthesis of indol-3-acetaldoxime and characterization of the compounds

All reagents were purchased from Sigma-Aldrich (Saint Louis, USA) and Acros (Waltham, MA, USA), and used as received, except for the deuterated solvents, which were purchased from Carlo-Erba. ^{1}H and ^{13}C NMR were recorded at 300 K in a Bruker Avance III 400 spectrometer, at 400 MHz and 101 MHz. Chemical shifts are given in ppm and were referenced using the residual signal from C*H*Cl_3 at 7.26 ppm and 77.16 ppm or C*H*$_3$OH at 3.31 ppm and 49.00 ppm for ^{1}H and ^{13}C, respectively [18]. H and C signals were assigned by *means* of ^{1}H,^{1}H-COSY and NOESY, as well as ^{1}H,^{13}C-HMBC experiments. IAOx was synthesized according to previously described methodologies [19–22] from indole-3-acetaldehyde (IAAld). Briefly, the IAAld was obtained as its bisulfite adduct after oxidation of Trp with sodium hypochlorite. The free aldehyde was released upon treatment of the bisulphite adduct with sodium carbonate, and despite its low stability in solution, it was satisfactorily characterized by NMR (see below). The free aldehyde was further reacted with an excess of hydroxylamine to provide IAOx in good yields (*ca.* 70%) as a mixture of *Z* and *E* isomers. An enriched IAOx sample in *E* isomer was obtained after recrystallization in methanol. The presence of *E* and *Z* isomers was confirmed by UPLC. UPLC-MS$^+$ spectra were recorded in a UPLC-QTOF spectrometer model Acquity SYNAPTTM G2 HDMS (Waters, USA) at the *Servicio Central de Análisis de Bizkaia (SGIker)* at the Facultad de Ciencia y Tecnología, Universidad del País Vasco, Leioa, Spain.

An Aquity UPLC BEH C18 column (1.7 µm, 2.1x 50 mm, Waters P/N 186002350) was used as the stationary phase with a mobile phase of solvent A (water with 0.1% v/v formic acid) and B (water with 5% MeOH and 0.1 % formic acid) at 30ºC, and with a constant flux of 0.5 mL per min. A gradient of increasing concentration of B was used from 0% to 100% over 2.5 min (Supplementary Fig. 1). An MS spectrum of $[M+H]^+$: 175.0883 (expected 175.0866) was recorded (Supplementary Fig. 2).

The characterization of IAAld and IAOx by NMR provided the following spectral parameters, where 'in' refers to indole:

2.2. Indole-3-acetaldehyde (IAAld)

^{1}H NMR ($CDCl_3$, δ, ppm): 9.78 (1H, t, J= 2.57 Hz, C*H*O), 8.17 (1H, b, N*H*), 8.07 (1H, dd, J= 8.07, 0.98 Hz, H6in), 7.40 (1H, dt, J= 8.13, 0.88 Hz, H5in), 7.24 (1H, ddd, J= 8.31, 7.33 1.22, H4in), 7.18-7.14 (2H, m, H2in, H7in), 3.82 (2H, dd, J= 2.51, 0.79 Hz, CH_2) (Supplementary Fig. 3)

^{13}C{^{1}H}NMR ($CDCl_3$, δ, ppm): 199.52 (*C1*), 136.26 (C7a.in), 127.40 (C3a.in), 123.35 (C2in), 122.61 (C6in), 120.01 (C5in), 118.53 (C4in), 111.33 (C7in), 106.22 (C3in), 40.36 (C_2) (Supplementary Fig. 4)

2.3. Indole-3-acetaldoxime (IAOx)

Z isomer: ^{1}H NMR (CD_3OD, δ, ppm): 7.51 (1H, dt, J= 7.94, 0.95 Hz, *H4in*), 7.34 (1H, dt, J= 8.14, 0.87 Hz, *H7in*), 7.12-7.08 (2H, m, *H2in, H6in*), 7.00 (1H, dddd, J= 7.1, 1.04, 0.92, 0.92 Hz, *H5in*), 6.79 (1H, t, J= 5.03 Hz, C_HNOH), 4,60 (1H, b), 3.80 (2H, dd, J= 5.30, 0.86, CH_2) (Supplementary Fig. 5)

^{13}C{^{1}H}NMR (CD_3OD, δ, ppm): 152.22(*C1)*, 138.34 (*C7a.in*), 128.75 (*C3a.in*), 123.83 (*C2in*), 122.65 (*C6in*), 119.89 (*C5in*), 119.32 (*C4in*), 112.42 (*C7in*), 111.18 (*C3in*), 22.43 (*C2)* (Supplementary Fig. 6)

E isomer: ^{1}H NMR (CD_3OD, δ, ppm): 7.54 (1H, dt, J= 8.00, 1.01 Hz, *H4in*), 7.48 (1H, t, J= 5.86 Hz, C*H*NOH), 7.33 (1H, dt, J= 8.14, 0.87 Hz, *H7in*), 7.12-7.08 (2H, m, *H2in, H6in*), 6.99 (1H, dddd, J= 7.1, 1.04, 0.92, 0.92 Hz, *H5in*), 3.60 (2H, dd, J= 6.40, 0.88, CH_2) (Supplementary Fig. 7)

$^{13}C\{^{1}H\}$NMR (CD_3OD, δ, ppm): 151.54 (*C1)*, 138.36 (*C7a.in*), 128.77 (*C3a.in*), 123.81 (*C2in*), 122.67 (*C6in*), 119.89 (*C5in*), 119.47 (*C4.in*), 112.41 (*C7in*), 110.99 (*C3in*), 26.98 (*C2)* (Supplementary Fig. 8).

2.4. The plant growth system, experimental set up and sampling

Seeds of *Medicago truncatula* Gaertn. ecotype *Jemalong* were scarified with 95% sulfuric acid for 8 min, then washed with sterile water and further surface sterilized with 50% sodium hypochlorite for five minutes, followed by a new wash with sterile water until the pH reached 7. The seeds were subsequently germinated on 0.4 % agar (w/v) plates at 14 ºC in darkness for 72 h. Four germinated seeds were transferred in a sterile laminar flow cabinet into each Petri plate containing 100 ml of Fahraeus medium with 5 g l^{-1} of phytagel as a nutrient medium as explained in [23]. The NO_3^--, NH_4^+- or urea-containing growth media were prepared at 1 mM of N, and they were applied as described in [23]. This concentration was selected as non-limiting for N availability based on previous results[23]. A trial experiment to determine an adequate IAOx concentration (1 µM, 5 µM, 25 µM, 100 µM and 200 µM) was performed (Fig. 1) and from this, the 200 µM IAOx concentration was selected (see results for more details). After 1 day of growth, 10 µM IAA or 200 µM IAOx or both diluted in DMSO were added to each of the media once the temperature dropped below 40ºC. As IAA and IAOx were diluted in DMSO, 0.25 µL/ml of DMSO were added to each non-hormone medium to ensure that all treatments contained the same amount of DMSO. Plants were grown in a growth chamber for 14 days at a day/night temperature of 24.5/22 ºC, with 80% relative humidity, a 16/8 h day/night photoperiod and 70 µmol m^{-2} s^{-1} of photosynthetically active radiation. Harvesting was always conducted 6 h after the light period onset. Five randomly selected plants from different pots were collected; shoots and roots were separated, weighed, and then frozen in liquid N_2, being stored at -80 ºC for further analyses.

For gene expression analysis, germinated seeds were grown for 4 days with NO_3^--, NH_4^+- or urea-containing growth media and then seedlings were incubated for two hours in the same media containing 200 µM of IAOX.

2.5. Root growth and root system architecture (RSA) *determination*

Root growth quantification and architecture characterization were performed with the semi-automated image analysis software Image J [24] using the SmartRoot plugin [23] [25]. The root system was photographed (2D photographs) every 2 days for 14 days. A dataset of approximately 1000 pictures containing architectural descriptions of the RSA under the

different treatments was established. For simpler comprehension of whether the plant-root architecture resembled the "superroot" phenotype, [26], the "superroot index" (SRI) was established. This index represents the ratio between the numbers of lateral-roots and the main-root length in cm. The sum of elongation, the total surface area covered by the roots, and the volume of every plant root and plate were analysed as previously described [23].

2.6. Gene expression analysis.

RNA was extracted from 20 mg of frozen seedling powder with a Nucleospin RNA plant kit (Macherey-Nagel, Dürem, Germany), which includes the DNAse treatment. One µg of RNA was retrotranscribed into cDNA (PrimeScriptTM RT; Takara Bio Inc.).

To select *M. truncatula* genes encoding for Aldehyde oxidase and CYP71A, a BLAST analysis was performed in the GenBank (https://www.ncbi.nlm.nih.gov/), phytozome (https://phytozome.jgi.doe.gov/) and Uniprot (https://www.uniprot.org/) databases using as query sequences *Arabidopsis thaliana* Aldehyde Oxidase 1 (AT5g20960) and CYP71A13 (AT2G30770). With this approach, two *Medicago truncatula* genes encoding for aldehyde oxidases were found (*Medtr5g087410* and *Medtr5g087390*) and two genes (*Medtr4g104540* and *Medtr4g104550*) were selected that are among the closest *M. truncatula* orthologues of *Arabidopsis* CYP71A13. The primers used were as described in Table S9.

Gene expression was determined from 2 µL of cDNA diluted 1:10 in a 15 µL reaction volume using SYBR Premix ExTaqTM (Takara Bio Inc.) in a Step One Plus Real Time PCR System (Applied Biosystems). The PCR program was: 95 °C for 5 min, 40 cycles of 15 s at 94 °C followed by 1 min at 60 °C, and a final melting curve was programmed. Relative gene expression was calculated as the ΔCt between each gene and the average of the housekeeping genes. *Ubiquitin carrier protein 4* and *26S proteasome regulatory subunit S5A_2* were used as housekeeping genes ([27]Ref). The absence of contamination with genomic DNA was confirmed by the melting curve in all the RNA samples.

2.7. Extraction and determination of IAA, IAOx and indole-3- acetonitrile (IAN)

The extraction protocol was adapted from a previously reported method [23]. Approximately 0.2 g of frozen plant tissue was ground to powder in a mortar with liquid N_2 and then homogenized with 5 ml of a solution of methanol:H_2O (80:20, v/v) stabilized with BHT (200 $mg \cdot L^{-1}$), and then transferred to a 50 mL centrifuge tube with the addition of indole propionic

acid as internal standard. Samples were shaken for 1 hour at room temperature. The solids were separated by centrifugation at 10800 g for 10 min and re-extracted for 20 min with an additional 2 mL of extraction media. The supernatants were pooled and concentrated by rotary distillation to approximately 1 mL. The extract was combined with 1 mL of acetic 0.4% v/v acid/H_2O (*HAcW*) and eluted with 20 mL of CH_3OH: *HAcW* 70:30 (v/v) in a reversed phase Sep-Pak C18 silica cartridge (6 mL, 500 mg, 55-105 µm particle size (WAT043395, Waters, USA) previously conditioned with 5 mL of CH_3OH, and 5 mL of *HAcW*. The methanol was evaporated by rotary distillation until only water was left, then 0.5 mL of 1 M formic acid was added. The resulting solution was extracted with diethyl ether (2 x 5 mL each) and the organic layers were recovered; the solvent was removed under reduced pressure and finally, the residue was dissolved in 200 µL of *HAcW*/Methanol/acetonitrile (49:21:30).

HPLC coupled to a fluorescence detector was performed using a Waters 575 HPLC Pump (Waters, USA) controlled by a Waters Pump Control Module (Waters, USA) and a Waters 474 fluorescence detector (Waters, USA). A µBondapak C18 column (10 µm 125 Å 3.9 x 150 mm, WAT86684 Waters, USA) was used as stationary phase, with a mobile phase of solvent A (water with 0.4% v/v acetic acid) and B (acetonitrile), with a constant flux of 0.5 mL per min. A gradient-increasing concentration was used for solvent B, from 20% to 40 % for 25 min and then remained constant for 10 min. The concentration of B was then gradually decreased to 20% for 5 min and allowed to rest for additional 5 min. The fluorescence detector was set at λ_{ex}=280 nm λ_{em}= 331 nm with a gain of 10. Retention times were 13.98 min for IAA, 15.4 min for the first isomer of IAOx, 17.87 min for the second isomer of IAOx, 18.77 min for the internal standard (indole propionic acid) and 19.98 min for IAN (Supplementary Figure 9)

2.8. Statistics

Differences among treatments were tested with one-way ANOVA and the Student-Newman-Keuls *post-hoc* test (Fig. 2-7). For figure 8 differences between control and treatments were tested with Student t test. All data were tested for normality (Kolmogorov-Smirnof test) and homogeneity of variances (Cochran test) and log-transformed if necessary. When this test failed to meet ANOVA assumptions, the data were analysed using the non-parametric Mann-Whitney test. The resulting p-values were considered statistically significant at $\alpha = 0.05$. Statistical analyses were performed with IBM SPSS Statistics for Windows, Version 24.0. Armonkm NY: IBM Corp**.**

3. Results

IAOx was chemically synthesized starting from indole-3-acetaldehyde that had been obtained in its bisulfite adduct from Trp. The structure of the IAOx molecule was confirmed by MS and NMR analysis. NMR analysis evidenced that IAOx, as expected, was obtained as a mixture of the two geometrical isomers, *Z* and *E*. Recrystallization in methanol allowed us to obtain an enriched mixture of E-isomer. No traces of indole-3-acetaldehyde or indole-3-acetic acid were detected by NMR (Supplementary Fig. 3 and 5). The purity of the synthesized IAOx was also assessed by UPLC-ESI+, injecting a solution of IAOx in TRIS buffer and analysing it by UPLC-ESI+. Thus, besides the residual signals from the solvent and one compound arising at 1.81 min from the hydroxylamine–TRIS exchange on the carbonyl compound (Supplementary Fig. 7), only two compounds were detected whose mass corresponded to that of the IAOx *E* and *Z* isomers.

Regarding the phenotypes, We established first that the external application of IAOx to the plant solid medium was able to induce the "superroot" phenotype in *M. truncatula* plants [9,10]. To achieve this target, the main root growth rate and the number of lateral roots at different IAOx concentration were evaluated in seedlings of *M. truncatula* grown on NO_3^- for 15 days with different doses of IAOx (Fig. 1). The results showed that when using low doses of IAOx (1, 5 and 25 µM), growth of the main root was elongated, while higher IAOx concentrations (100 and 200 µM) induced a strong reduction in the main root growth (Fig. 1A). The "superroot" index (SRI, see Materials and Methods), which relates the plant root shape to the "superroot" phenotype (Fig. 1B), was higher when IAOx doses were increased. Based on these results, the 200 µM IAOx dose was selected as being effective at inhibiting the elongation of the main root and to obtain a "superroot" phenotype. On the other hand, the 10 µM IAA dose was selected, because that has been shown to induce a strong signalling effect [28].

The standard effect of IAOx on the *M. truncatula* root phenotype under different NO_3^-, NH_4^+ and urea nutrition can be visualized in Fig. 2. Plants grown in NH_4^+ and urea exhibited a lower main root elongation (expressed as main root length at a given day minus the main root length at day=0) than those grown in NO_3^- (Fig. 3). Despite this, all non-treated plants showed a stable growth over time, although with different final elongations, which were ≈ 7, 4.5 and 5 cm for the NO_3^-, NH_4^+ and urea treatments, respectively (Fig. 3). When IAA, IAOx or the two combined were applied, the average main root elongation was greatly diminished in the three N nutrition types (Fig. 3), although for NO_3^-nutrition the reduction in the main root elongation was less pronounced (Fig. 3A). Besides, in NO_3^--grown plants, either IAA- or IAOx-treated

plants had a similar final main root growth but divergent elongation behaviour (Fig. 3A). Nevertheless, when both IAA and IAOx were applied together, the inhibitory effect was even stronger, nearly fully inhibiting main root elongation during the 14 days of the experiment (Fig. 3A). Conversely, plants grown using NH_4^+ or urea as an N source showed a strong inhibitory effect on main root elongation under all treatments (IAA, IAOx, IAA+IAOx) (Fig. 3B, C). Moreover, IAOx and/or IAA application initiated significant changes in the main root surface (Fig. 3D, E, F). Firstly, in NO_3^--grown seedlings IAOx induced the largest surface changes, especially during the initial developmental stages (Fig. 3D). Secondly, under NH_4^+ nutrition, the combined effect of IAA and IAOx was stronger than each compound used separately (Fig. 3E). Furthermore, in the early growth stages, a 10-fold increase in the main root surface area of plants treated with both IAOx and IAA compared to non-treated plants was observed (Fig. 3E). Thirdly, under urea nutrition all treatments (IAA, IAOx and the combination of both) increased the main root surface area of the plants, but with no significant differences among treatments (Fig. 3F). Regarding the main root volume, NO_3^- nutrition was significantly more influenced by the hormonal treatments compared to the other nutrition types, and under the IAA and IAOx combination it showed more pronounced effects on days 12 and 14 (Fig. 3G).

The lateral root length data is presented in Fig. 4A-C as the sum of all lateral root lengths of a given plant. The data showed that NH_4^+ and urea control plants exhibited shorter lateral roots than plants grown under NO_3^- control nutrition. Additionally, IAOx significantly induced longer lateral roots than the IAA-treated plants under NO_3^- (Fig. 4A) and NH_4^+ nutrition (Fig. 4B). Moreover, under these two N sources, lateral root lengths were longer when IAOx was combined with IAA (Fig. 4A, B), whereas IAOx-treated urea-grown plants showed similar lateral roots length to control plants (Fig. 4C). On the other hand, NH_4^+-grown control plants exhibited a higher number of lateral roots (Fig 4E) compared to the NO_3^-or urea control plants. More remarkably, the IAOx treatment boosted the lateral root number in the initial days of the treatment (Fig. 4D, E, F), while under NO_3^- or urea nutrition IAA induced no significant differences in the number of lateral roots (Fig. 4D, F). Furthermore, under NH_4^+ nutrition, IAA application almost completely inhibited lateral roots (Fig. 4E). In contrast, under all N nutrition types, when IAA was combined with IAOx no inhibiting effect was observed (Fig. 4D-F). When IAA and IAOx were applied under urea nutrition, there was a slight increase in the number of lateral roots, although this was not significant (Fig. 4F). Regarding the surface area and volume of lateral roots, IAOx enhanced both parameters under the three types of N nutrition (Fig. 4G-L). However, the application of both molecules combined affected lateral

306 root volumes and surface areas differentially, depending on the N source. Thus, while
307 IAOx+IAA under NH_4^+ nutrition induced the largest increase in lateral root surface and volume
308 (Fig. 4H, K), IAOx alone strongly increased the volume and surface in urea-grown seedlings
309 (Fig. 4I, L). In addition, IAOx+IAA increased the lateral root surface under NO_3^- nutrition (Fig.
310 4J), although no significant differences in the lateral root volume were observed between IAOx
311 and IAOx+IAA treatments (Fig. 4G).

312 The SRI was analysed for the treatments and N nutrition during the study. The SRI index
313 showed the greatest increase in the IAOx+IAA-treated plants, especially in seedlings grown
314 under NO_3^- (Fig. 5A). The combined treatment increased the SRI in NH_4^+-grown plants
315 exclusively during the initial growth stages, while in the last days of the experiment IAOx-
316 treated plants showed similar increased SRIs to the combined-treatments. Remarkably, at the
317 end of the experiment (from day 12) the SRI was significantly lower in IAA-treated plants
318 compared to the IAOx-treated ones (Fig. 5B). Nevertheless, all urea-grown treated seedlings
319 (with IAA, IAOx or IAOx+IAA) showed an increase in the SRI, and this was also slightly
320 higher for plants treated with both IAOx and IAA during the final growth stages (Fig.4C).
321 The IAOx, IAA and IAN contents were analysed by HPLC-fluorescence in roots and
322 shoots (Figs. 6-7), not only to confirm that the exogenous compounds were entering plant cells,
323 but also to check for potential processing and transport of IAA and IAOx. Endogenous contents
324 of IAOx in plants without IAOx supplementation were surprisingly high in the roots of NO_3^-
325 and urea-grown plants, with the lowest value found in NH_4^+ grown roots (Fig. 6D). On the
326 other hand, IAA levels were significantly higher in the shoots of NO_3^- grown plants than in the
327 roots of NH_4^+-or urea-grown plants (Fig. 6C). However, IAN contents were not significantly
328 different (Fig. 6 B, E). When IAOx was applied externally, substantially higher IAOx and IAN
329 contents were found in the shoots of plants grown in the NO_3^- medium (Fig. 7A, B). Indeed,
330 NO_3^- plants treated with IAOx showed a 9-fold increase in their IAOx shoot content (Fig. 7A)
331 compared to plants grown without IAOx supplementation (Fig. 6A). In contrast, the IAA levels
332 in shoots of plants grown in the three N sources fell by approximately one third after IAOx
333 application (Fig. 7C, 6C). Regarding the contents inside the roots, the IAOx levels increased
334 in IAOx-supplemented plants grown in either NH_4^+ or urea (Fig. 7D) compared to the IAOx
335 root content in non-supplemented plants (Fig. 6D). Conversely, the IAOx content decreased in
336 NO_3^- grown plant roots supplemented with IAOx relative to those without the IAOx
337 supplement (Figs. 7D, 6D). Regarding IAA content, when plants were supplemented with
338 IAOx the IAA content decreased in all shoots and in NO_3^--grown plant roots to levels that were

below those recorded when no IAOx supplementation was present (Fig. 6F). Interestingly, two-hour IAOx treatment produced a high level of induction (10x to 60x fold change) in the *CYP71A* genes, which are potentially responsible for IAOx→IAN conversion (Fig. 8B). Even though the expression of these genes was present in all the nutrition types, the greatest increase was observed in NH_4^+-grown plants while NO_3^--grown plants showed the lowest induction (Fig. 8.B). In contrast, the aldehyde oxidase genes involved in the IAAld→IAA pathway showed no induction after IAOX addition (Fig. 8 C) for every nutrition type.

4. Discussion

4.1 The differential effect of IAOx and IAA.

IAOx promotes the elongation of the main root at very low concentrations, but the SRI does not change until higher doses are applied ($\geq$ 100µM). This greater elongation under low IAOx concentrations may be due to metabolic conversion of the IAOx to IAA, which exerts its effects at very low concentrations [29]. Only when the balance is altered, and significant amounts of IAOx accumulate, the effect of IAOx itself can be observed. This effect at high IAOx concentrations is clearly different from IAA at high concentrations (not shown).

IAOx has always been described as a non-accumulated intermediate compound in the Trp-IAA pathway of cruciferous plants [2], although its presence has been proposed in the non-cruciferous plant maize [29]. In contrast, our results show that not only does IAOx accumulate in the tissues of plants from a non-Brassicaceae plant like the legume *M. truncatula* (Figs. 5, 6), but we also show that IAOX accumulates in this species in high amounts in shoots (up to 20 ng/mg FW) (Fig 5. A) and roots (up to 100 ng/mg FW) (Fig .5 D). This might be due to the IAOx extraction protocol applied here, which is more sensitive for detecting low amounts of IAOx, and also IAA, in plant extracts.

IAOx contents are modulated depending on the type of N source provided (Fig. 6), reaching much higher levels than those found in *A. thaliana* [17]. In addition, these results also verified that the seedlings grown in media supplemented with IAOx were able to internalize and process the added IAOx (Fig. 7). Our data showed that IAOx may be largely transported from roots to shoots in $_{Ox}NO_3^-$-grown *M. truncatula* and, to a lesser extent, in $_{Ox}$urea- and $_{Ox}NH_4^+$-grown plants. Under NH_4^+ nutrition, we found that the endogenous IAOx contents in roots were lower than those under NO_3^- or urea nutrition (Fig. 6). However, when IAOx was added externally, the IAOx internal contents significantly increased under NH_4^+ and were reduced under NO_3^-

(Fig. 7). All this data suggests that transport of IAOx may occur from roots to shoots as a potential compensation mechanism, which was especially evident in NO_3^--grown plants. Also, it seems quite probable that IAOx competes with IAA for transporters such as PIS1, known to transport auxin compounds, including its precursors [6,30]. Furthermore, the IAOx may well be processed in a similar way to IAA for degradation and storage, and we cannot rule out that IAOx supplementation induced these degradation and storage mechanisms in the plants to remove excess auxinic compounds.

IAOx has been described as an important metabolic switch between IAA and glucosinolate production [2]. However, IAOx-dependent IAA biosynthesis is not as important as the indolepyruvic acid (IPyA) intermediated pathway for the synthesis of IAA, at least in the Brassicaceae (Zhao et al. 2002). On the other hand, under high-temperature conditions the micro RNA miR10515 triggers IAOx-dependent IAA biosynthesis by repressing the expression of SUR1 [2]. Further, a SUR1 mutant led to IAOx accumulation, thus enhancing IAA production [31]. Although *M. truncatula* roots presented superroot phenotypes when IAOx was added to the medium (Fig. 5), the IAA content did not increase (Fig. 7), supporting the concept that IAOx possesses a signalling effect by itself. Moreover, even though enhanced IAA production in mutant bacteria has been reported following accumulation of IAOx [32], our data do not indicate that IAOx is implicated in such a role under our experimental conditions. Altogether, our data point towards IAA synthesis being more complex than a direct pathway from IAOx, and that the IAA signalling crossroad is somehow modulated by addition of IAOx.

4.2 The signalling role of IAA and IAOx in relation to the type of nitrogenated nutrition

It is known that plants like *A. thaliana*, when grown with NH_4^+ or urea as the sole N source, may suffer NH_4^+ toxicity syndrome [15]. The IAA oxidase gene (*IAA-Ox*), which regulates cell IAA levels *in A. thaliana,* is among the numerous genes that are stress-regulated [33]. Thus, *IAA-Ox* expression may have controlled IAA levels within our studied plant roots, and this explains why our plants grown with NH_4^+ or urea as the N source showed no increase in their IAA levels. Nevertheless, their IAOx and IAN levels, which are intermediary compounds on the IAA biosynthesis pathway, did increase [6]. Indeed, when IAOx was added externally, the IAOx, IAN and IAA contents in *M. truncatula* plants grown with NO_3^-, a non-stressful N source for *M. truncatula* [15], remained low in the roots but became significantly high in the

shoots. This evidences that an excessive amount of IAOx in roots can block the transport of auxins from the upper tissues. However, the transport of IAOx and IAN to the shoot from the root cannot be discarded, because short distance upwards transport has been reported in pea plants [30]. The lower IAA contents could also be explained by the boosting of IAA degradation, via *IAA-Ox*, or conjugation triggered by IAOx, or as a regulatory mechanism of the plant response to the hormone imbalance [6].

Our data indicates that external IAOx application inhibits the main root development, including changes in length, surface and volume parameters. This result was especially relevant during the initial days of growth when hormonal regulation is critical. The decrease in elongation of the main root may relate to the observed drop in IAA content in shoots for all nutrition types when IAOx is supplied (Figs. 6 and 7). This reduction in elongation of the main root associated with a decrease in IAA has been observed previously in NH_4^+-grown plants when compared to NO_3^-grown plants [23]. In the present work, the changes in surface area and volume of the main roots were substantial. Under NO_3^- nutrition, IAOx boosted the surface area, unlike plants grown under NH_4^+, where only the combination of IAA+IAOx led to significant differences. The IAOx treatment induced a greater number of lateral roots than IAA in all the treatments, but its dependence on IAA was modulated through different nitrogen nutrition. As in NO_3^--grown plants, IAOx signals a greater number of secondary roots in the first days of growth (Fig. 4 D), and this difference is reduced in the following days. This can be explained by the regulation of IAA contents shown by the plants grown under NO_3^- and $_{Ox}NO_3^-$ as IAA seems to be reduced significantly in shoots and roots (Fig 6 C and 7 C). However, under NH_4^+ nutrition the hormonal treatments (IAA or IAOx alone) only seem to have reduced the number of lateral roots, and the recovery of the control phenotype only occurs when IAOx and IAA are combined (Fig. 4 E). Concomitantly, the IAA contents in roots were similar in NH_4^+ and $_{Ox}NH_4^+$ plants, and the major hormonal changes were seen in the IAOx and IAN contents (Fig. 6 and 7). This behaviour is concisely shown by the RSI (Fig. 5) and is also seen in the surface area and volume of the secondary roots (Fig. 4). These results not only show the important role of IAOx and IAA in root development signalling but the effect of IAOx itself and the important role it plays during IAA signalling. It is interesting that in terms of the lateral roots the mixtures of IAA + IAOx are nearly able to overcome the detrimental effects of NH_4^+ nutrition on the volume and surface area (Fig. 4). Additionally, when urea-grown plants are supplemented with IAOx they are able to recover surface and volume levels that match NO_3^--grown plants (Fig. 4). Overall, it seems that a deeper knowledge of the detailed function of auxins and auxin-

related compounds may help with some of the detrimental effects caused by the N source under some conditions.

The results of the expression levels measured for Cyp71A and aldehyde oxidase genes indicated that in *Medicago truncatula* the most important route for regulation of IAA synthesis from IAOx is probably the IAOx dehydratase pathway, which initially produces IAN and subsequently IAA via catalysis with nitrilase. Furthermore, the expression of aldehyde oxidase genes seemed insensitive to addition of IAOx and this may indicate an alternative function for this enzyme other than IAA synthesis from IAOx, at least at the stages studied. Moreover, the differences in expression levels found between nutrition types (Fig. 8B) are consistent with the IAN increases that we have measured *in planta* after 14 days of IAOx treatment, especially in roots (Fig. 7 E), thus evidencing the existence of this route in *M. truncatula* and its implication in IAA homeostasis and regulation. Nevertheless, the contents of IAA that are reduced in IAOx-treated plants relative to the untreated ones (Fig. 7 F) did not correlate with the gene expression and IAN amounts.

Importantly, the induction of Cyp71A genes is more marked under NH_4^+ nutrition than under NO_3^- nutrition, and point out to a more prominent role of the IAOx-dependent IAA synthesis under NH_4^+. This may be a mechanism plants deploy to compensate the overall lower IAA content observed in NH_4^+-grown *Medicago truncatula* plants (Fig. 6)[23]. Notably, previous results showed that only high IAA contents in the shoots significantly correlated with a better *M. truncatula* performance [23], as observed in NO_3^--grown plants (Fig. 6).

On the other hand, the distinct effects on plant architecture that were perceived after supplementation with IAOx or IAA+IAOx are more difficult to explain due to the compensatory metabolism of auxin mentioned before. Because IAOx modulates the IAA content (Fig.7), IAOx-treated plants may have less IAA available than those treated with a combination of IAOx and IAA, and this fits the reduced inhibition of the main root growth in these plants. Interestingly, the rise in IAN content observed in shoots (Fig 7. B), regardless of the nitrogen nutrition, is also observed in nitrilase-overexpressing mutants of *A. thaliana* [14]. The fact that this does not occur in NO_3^--fed plant roots correlates with the alterations in the auxin root-to-leaf transport due to changes in the NO_3^- transporter NRT1.1 [14]

Auxins are known to stimulate lateral root development, and NO_3^- has been proposed in their mechanisms of action [14]. It has also been suggested that nitric oxide (NO) may play a central

role in signalling lateral root formation by acting downstream of auxins [34]. For example, two *A. thaliana* mutants in the arginase isoenzyme genes, ARGAH1 or ARGAH2, which encode arginine amidohydrolase-1 and −2, respectively, exhibited a higher accumulation and efflux of NO and also doubled the number of lateral roots when exposed to exogenous naphthalene acetic acid, evidencing the importance of NO in auxin-mediated regulation [35]. Whether NO mediates the effect of IAOx is an interesting open question to solve. Further, auxin signalling during primary root growth has also been studied under NH_4^+ supplies by using the auxin-responsive reporter *DR5*::*GUS* in *Arabidopsis thaliana*. NH_4^+ nutrition induced a dramatic decrease in the response of the reporter to the synthetic auxin, naphthalene acetic acid, and the impaired root growth under NH_4^+ was partially rescued by exogenous auxin, suggesting that NH_4^+-induced nutritional and metabolic imbalances can be partially overcome by elevated auxin levels [36].

There are still uncertainties to solve regarding plant responses to supplementation with IAOx, because the effects on their RSA seem to be more powerful in the first stages of development. Although our spectral data for IAOx show that it is only able to absorb light within the UV range (data not shown), a certain amount of IAOx decay cannot be ruled out due to the extended periods of high light intensity experienced in the growth chamber. Also, plants are known to be very specific regarding the auxin signalling employed under any stress, and they use a plethora of mechanisms to regulate hormones [15,37,38]. Because our measures were made on day 14 of the experiment, we cannot exclude that regulation occurred in the days before harvest. Further analyses will be needed to conclude the nature of this response and/or regulation, and for dissecting the metabolism of the by-products in the plant.

5. Conclusions

Arabidopsis thaliana plants knocked down for the SUR genes displayed a “superroot” phenotype, which was proposed as being a consequence of higher amounts of IAA due to IAOx accumulation. We have found that in *M. truncatula* plants grown on an axenic medium with different nitrogen nutrition, application of the synthesized IAOx also induced the “superroot” phenotype, enhancing the number of secondary roots and the total surface covered by the roots, while IAOx induced shortening of the primary root. Our experiments also suggest an important interplay between IAA and IAOx, depending on the type of N nutrition. The IAA content measured in roots and shoots demonstrates that the effect of IAOx does not correlate with

changes in the contents of IAA, but it is due to a separate effect of IAOx or its derivative IAN. Although IAOx is supposed to be an intermediary compound that does not accumulate in tissue, we measured relatively high amounts of IAOx in *M. truncatula* in control conditions, indicating new insights for the pathway in this species. Our results shed new light onto the effect of a little-studied precursor of the auxin pathway, and open further questions about its role.

505 **Supplementary data**

506 Supplementary data are available at *Plant science* online in PDF.

507 Fig. S1. ^{1}H NMR spectrum for indole-3-acetaldehyde.

508 Fig. S2. ^{13}C NMR (APT sequence) spectrum for indole-3-acetaldehyde.

509 Fig. S3. ^{1}H NMR spectrum for indole-3-acetaldoxime (*Z* – isomer).

510 Fig. S4. ^{13}C NMR spectrum for indole-3-acetaldoxime (*Z* – isomer).

511 Fig. S5. ^{1}H NMR spectrum for indole-3-acetaldoxime (mixture of isomers).

512 Fig. S6. ^{13}C NMR (APT sequence) spectrum for indole-3-acetaldoxime (mixture of isomers).

513 Fig. S7. Indole-3-acetaldoxime (mixture of isomers) UPLC chromatogram.

514 Fig. S8. Indole-3-acetaldoxime (mixture of isomers) ESI^{+} spectrum.

515 Table S1. Primer sequences used in this study.

516

517 **References**

518 [1] J. Celenza, Metabolism of tyrosine and tryptophan-new genes for old pathways, Curr.
519 Opin. Plant Biol. 4 (2001) 234–240. doi:10.1016/S1369-5266(00)00166-7.

520 [2] W. Kong, Y. Li, M. Zhang, F. Jin, J. Li, A Novel Arabidopsis MicroRNA Promotes
521 IAA Biosynthesis via the Indole-3-acetaldoxime Pathway by Suppressing
522 SUPERROOT1, Plant Cell Physiol. 56 (2015) 715–726. doi:10.1093/pcp/pcu216.

523 [3] E. Glawischnig, B.G. Hansen, C.E. Olsen, B.A. Halkier, Camalexin is synthesized
524 from indole-3-acetaldoxime, a key branching point between primary and secondary
525 metabolism in Arabidopsis., Proc. Natl. Acad. Sci. U. S. A. 101 (2004) 8245–50.
526 doi:10.1073/pnas.0305876101.

527 [4] S. Sugawara, S. Hishiyama, Y. Jikumaru, A. Hanada, T. Nishimura, T. Koshiba, Y.
528 Zhao, Y. Kamiya, H. Kasahara, Biochemical analyses of indole-3-acetaldoxime-

dependent auxin biosynthesis in Arabidopsis, Proc. Natl. Acad. Sci. U. S. A. 106 (2009) 5430–5435. doi:10.1073/pnas.0811226106.

[5] K. Luck, J. Jirschitzka, S. Irmisch, M. Huber, J. Gershenzon, T.G. Köllner, CYP79D enzymes contribute to jasmonic acid-induced formation of aldoximes and other nitrogenous volatiles in two Erythroxylum species, (n.d.). doi:10.1186/s12870-016-0910-5.

[6] D. Olatunji, D. Geelen, I. Verstraeten, Control of endogenous auxin levels in plant root development, Int. J. Mol. Sci. 18 (2017). doi:10.3390/ijms18122587.

[7] N.D. Tivendale, J.J. Ross, J.D. Cohen, The shifting paradigms of auxin biosynthesis, Trends Plant Sci. 19 (2014) 44–51. doi:10.1016/j.tplants.2013.09.012.

[8] R.A. Korver, I.T. Koevoets, C. Testerink, Out of Shape During Stress: A Key Role for Auxin, Trends Plant Sci. 23 (2018) 783–793. doi:10.1016/j.tplants.2018.05.011.

[9] M.D. Mikkelsen, P. Naur, B.A. Halkier, Arabidopsis mutants in the C-S lyase of glucosinolate biosynthesis establish a critical role for indole-3-acetaldoxime in auxin homeostasis, Plant J. 37 (2004) 770–777. doi:10.1111/j.1365-313X.2004.02002.x.

[10] S. Bak, F.E. Tax, K.A. Feldmann, D.W. Galbraith, R. Feyereisen, CYP83B1, a cytochrome P450 at the metabolic branch point in auxin and indole glucosinolate biosynthesis in Arabidopsis., Plant Cell. 13 (2001) 101–11. doi:10.1105/tpc.13.1.101.

[11] M. Sauer, S. Robert, J. Kleine-Vehn, Auxin: Simply complicated, J. Exp. Bot. 64 (2013) 2565–2577. doi:10.1093/jxb/ert139.

[12] P.J. Davies, Plant hormones: Biosynthesis, signal transduction, action!, 2010. doi:10.1007/978-1-4020-2686-7.

[13] K. Ruzicka, L.C. Strader, A. Bailly, H. Yang, J. Blakeslee, L. Langowski, E. Nejedla,

H. Fujita, H. Itoh, K. Syono, J. Hejatko, W.M. Gray, E. Martinoia, M. Geisler, B. Bartel, A.S. Murphy, J. Friml, Arabidopsis PIS1 encodes the ABCG37 transporter of auxinic compounds including the auxin precursor indole-3-butyric acid, Proc. Natl. Acad. Sci. 107 (2010) 10749–10753. doi:10.1073/pnas.1005878107.

[14] G. Krouk, B. Lacombe, A. Bielach, F. Perrine-Walker, K. Malinska, E. Mounier, K. Hoyerova, P. Tillard, S. Leon, K. Ljung, E. Zazimalova, E. Benkova, P. Nacry, A. Gojon, Nitrate-regulated auxin transport by NRT1.1 defines a mechanism for nutrient sensing in plants, Dev. Cell. 18 (2010) 927–937. doi:10.1016/j.devcel.2010.05.008.

[15] R. Esteban, I. Ariz, C. Cruz, J.F. Moran, Review: Mechanisms of ammonium toxicity and the quest for tolerance, Plant Sci. 248 (2016) 92–101. doi:10.1016/j.plantsci.2016.04.008.

[16] N.K. Clay, A.M. Adio, C. Denoux, G. Jander, F.M. Ausubel, Glucosinolate metabolites required for an Arabidopsis innate immune response., Science. 323 (2009) 95–101. doi:10.1126/science.1164627.

[17] Y. Zhao, A.K. Hull, N.R. Gupta, K.A. Goss, J. Alonso, J.R. Ecker, J. Normanly, J. Chory, J.L. Celenza, Trp-dependent auxin biosynthesis in Arabidopsis: involvement of cytochrome P450s CYP79B2 and CYP79B3, Genes Dev. 16 (2002) 3100–3112. doi:10.1101/gad.1035402.

[18] G.R. Fulmer, A.J.M. Miller, N.H. Sherden, H.E. Gottlieb, A. Nudelman, B.M. Stoltz, J.E. Bercaw, K.I. Goldberg, NMR chemical shifts of trace impurities: Common laboratory solvents, organics, and gases in deuterated solvents relevant to the organometallic chemist, Organometallics. 29 (2010) 2176–2179. doi:10.1021/om100106e.

[19] F. Hofmann, T. Rausch, W. Hilgenberg, Preparation of radioactively labeled indole-3-

acetic-acid precursors, J. Labelled Comp. Radiopharm. 18 (1981) 1491–1495. doi:10.1002/jlcr.2580181014.

[20] A. Ahmad, I.D. Spenser, Indolyl-3- pyruvic acid oxime as the precursor of indolyl-3-acetonitrile, Can. J. Chem. Can. Chim. 38 (1960) 1625–1634. doi:10.1139/v60-223.

[21] R.A. Gray, Preparation and properties of 3-indoleacetaldehyde, Arch. Biochem. Biophys. 81 (1959) 480–488. doi:10.1016/0003-9861(59)90228-0.

[22] E. Glawischnig, B.G. Hansen, C.E. Olsen, B.A. Halkier, Camalexin is synthesized from indole-3-acetaldoxime, a key branching point between primary and secondary metabolism in Arabidopsis, PNAS. 101 (2004) 8250–8425. doi:10.1073/pnas.0305876101.

[23] R. Esteban, B. Royo, E. Urarte, Á.M. Zamarreño, J.M. Garcia-Mina, J.F. Moran, Both Free Indole-3-Acetic Acid and Photosynthetic Performance are Important Players in the Response of Medicago truncatula to Urea and Ammonium Nutrition Under Axenic Conditions, Front. Plant Sci. 7 (2016) 140. doi:10.3389/fpls.2016.00140.

[24] J. Schindelin, I. Arganda-Carreras, E. Frise, V. Kaynig, M. Longair, T. Pietzsch, S. Preibisch, C. Rueden, S. Saalfeld, B. Schmid, J.-Y. Tinevez, D.J. White, V. Hartenstein, K. Eliceiri, P. Tomancak, A. Cardona, Fiji: an open-source platform for biological-image analysis, Nat Meth. 9 (2012) 676–682. doi:10.1038/nmeth.2019.

[25] G. Lobet, M.P. Pound, J. Diener, C. Pradal, X. Draye, C. Godin, M. Javaux, D. Leitner, F. Meunier, P. Nacry, T.P. Pridmore, A. Schnepf, Root system markup language: toward a unified root architecture description language., Plant Physiol. 167 (2015) 617–27. doi:10.1104/pp.114.253625.

[26] W. Boerjan, M.T. Cervera, M. Delarue, T. Beeckman, W. Dewitte, C. Bellini, M. Caboche, H. Van Onckelen, M. Van Montagu, D. Inzé, Superroot, a recessive mutation

in Arabidopsis, confers auxin overproduction., Plant Cell. 7 (1995) 1405–19. doi:10.1105/TPC.7.9.1405.

[27] E. Urarte, A.C. Asensio, E. Tellechea, L. Pires, J.F. Moran, Evaluation of the anti-nitrative effect of plant antioxidants using a cowpea Fe-superoxide dismutase as a target, Plant Physiol. Biochem. 83 (2014) 356–364. doi:10.1016/j.plaphy.2014.08.019.

[28] P.E. Pilet, M. Saugy, Effect on Root Growth of Endogenous and Applied IAA and ABA: A Critical Reexamination., Plant Physiol. 83 (1987) 33–38. doi:10.1104/pp.83.1.33.

[29] J.G. and T.G.K. Sandra Irmisch, Philipp Zeltner, Vinzenz Handrick, The maize cytochrome P450 CYP79A61 produces phenylacetaldoxime and indole-3-acetaldoxime in heterologous systems and might contribute to plant defense and auxin formation, BMC Plant Biol. 15 (2015) 128. doi:10.1186/s12870-015-0526-1.

[30] K. Ruzicka, L.C. Strader, A. Bailly, H. Yang, J. Blakeslee, L. Langowski, E. Nejedla, H. Fujita, H. Itoh, K. Syono, J. Hejatko, W.M. Gray, E. Martinoia, M. Geisler, B. Bartel, A.S. Murphy, J. Friml, Arabidopsis PIS1 encodes the ABCG37 transporter of auxinic compounds including the auxin precursor indole-3-butyric acid, Proc. Natl. Acad. Sci. 107 (2010) 10749–10753. doi:10.1073/pnas.1005878107.

[31] S. Sugawara, S. Hishiyama, Y. Jikumaru, A. Hanada, T. Nishimura, T. Koshiba, Y. Zhao, Y. Kamiya, H. Kasahara, Biochemical analyses of indole-3-acetaldoxime-dependent auxin biosynthesis in Arabidopsis, Proc. Natl. Acad. Sci. U. S. A. 106 (2009) 5430–5435. doi:https://doi.org/10.1073/pnas.0811226106.

[32] M.D. Mikkelsen, C.H. Hansen, U. Wittstock, B.A. Halkier, Cytochrome P450 CYP79B2 from Arabidopsis Catalyzes the Conversion of Tryptophan to Indole-3-acetaldoxime, a Precursor of Indole Glucosinolates and Indole-3-acetic Acid, (2000).

624 doi:10.1074/jbc.M001667200.

625 [33] J. Xu, W. Wang, H. Yin, X. Liu, H. Sun, Q. Mi, Exogenous nitric oxide improves
626 antioxidative capacity and reduces auxin degradation in roots of Medicago truncatula
627 seedlings under cadmium stress, Plant Soil. 326 (2010) 321–330. doi:10.1007/s11104-
628 009-0011-4.

629 [34] M. Yu, L. Lamattina, S.H. Spoel, G.J. Loake, Nitric oxide function in plant biology: A
630 redox cue in deconvolution, New Phytol. 202 (2014) 1142–1156.
631 doi:10.1111/nph.12739.

632 [35] T. Flores, C.D. Todd, A. Tovar-Mendez, P.K. Dhanoa, N. Correa-Aragunde, M.E.
633 Hoyos, D.M. Brownfield, R.T. Mullen, L. Lamattina, J.C. Polacco, Arginase-negative
634 mutants of Arabidopsis exhibit increased nitric oxide signaling in root development.,
635 Plant Physiol. 147 (2008) 1936–46. doi:10.1104/pp.108.121459.

636 [36] H. Yang, J. von der F.-B. Jiří Friml, J.U. Lohmann, B. Neuhäuser, U. Ludewig, Auxin-
637 modulated root growth inhibition in Arabidopsis thaliana seedlings with ammonium as
638 the sole nitrogen sourcee, Funct. Plant Biol. 42 (2014) 239–251.
639 doi:https://doi.org/10.1071/FP14171.

640 [37] B.G. Forde, Nitrogen signalling pathways shaping root system architecture: an update,
641 Curr. Opin. Plant Biol. (2014) 30–36. doi:10.1016/j.pbi.2014.06.004.

642 [38] J.K.H. Jung, S. Mccouch, A.E. Stapleton, B.J. Janssen, M. Bennett, Getting to the
643 roots of it: genetic and hormonal control of root architecture, Front. Plant Sci. 618
644 (2013) 58–1. doi:10.3389/fpls.2013.00186.

645

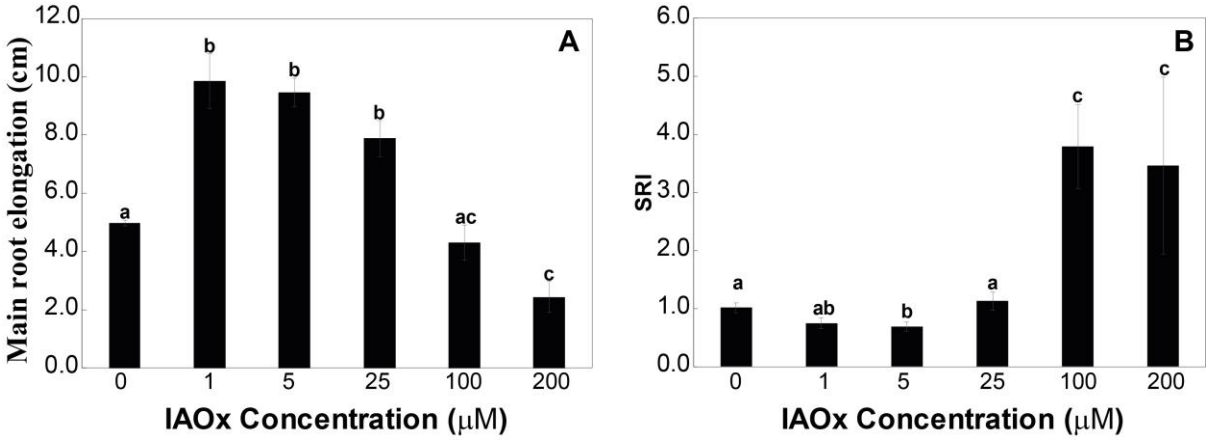

646

647 Fig. 1. Effect of IAOX concentrations (0, 1, 5, 25, 100 and 200 µM) on main root elongation
648 (cm) (A) and the effect of IAOx on the "superroot index" (SRI) (B) in *M. truncatula* seedlings
649 grown for 14 days under 1mM of NO_3^-. The bars indicate the means of 15-20 replicates ± S.E.
650 An analysis of variance was performed considering concentration as a fixed factor. Different
651 superscripted letters denote statistically significant differences at α =0.05 using Student-
652 Newman-Keuls tests.

653

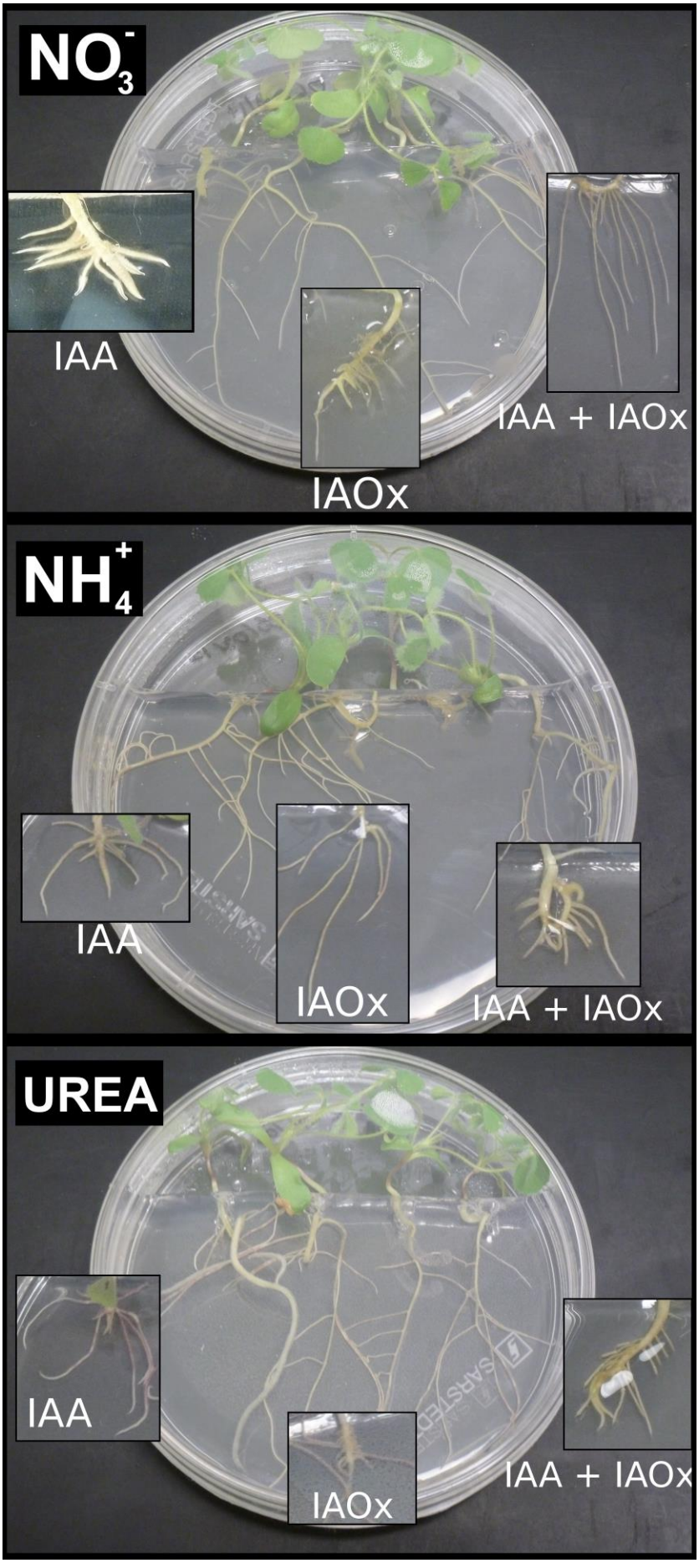

Fig. 2. A representative image of *M. truncatula* roots grown under NO_3^-, NH_4^+ or urea at day 14 is shown (controls). Next to each control are representative images of seedlings grown with the addition of IAA, IAOx or IAOx + IAA.

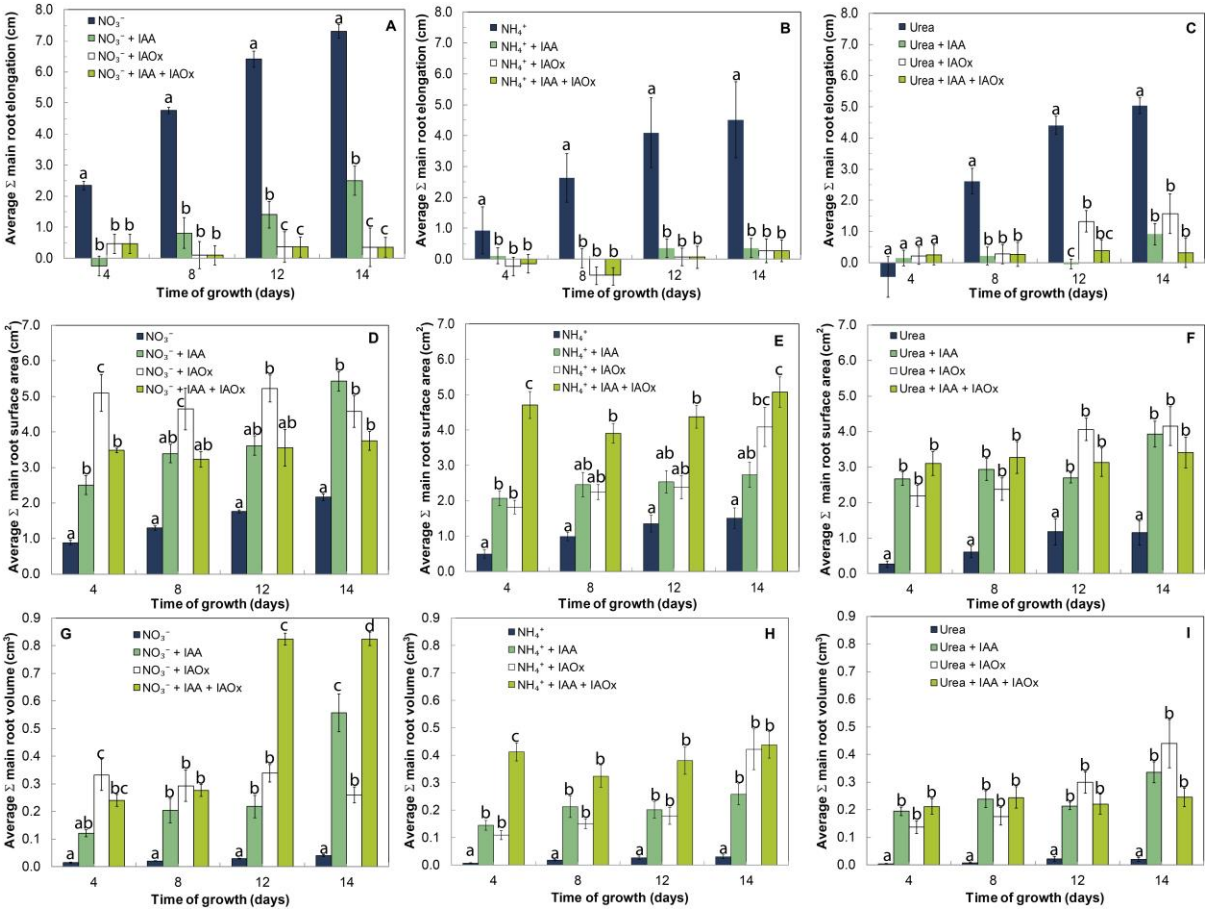

665

666 Fig. 3. Effect of IAOx, IAA and the combination of both on the elongation of the main root
667 (cm), surface area (cm^2) and volume (cm^3) of *M. truncatula* seedlings grown for 14 days under
668 1mM of NO_3^- (A, D, G), NH_4^+ (B, E, H) or urea (C, F, I). The values are the mean of 15-20
669 replicates ± S.E. An analysis of variance was performed considering the treatment as a fixed
670 factor. Asterisks in panels A, C and E indicate significant differences (α =0.05) between
671 treatments. In the rest of the panels, different superscripted letters denote statistically
672 significant differences at α =0.05 using Student-Newman-Keuls tests.

673

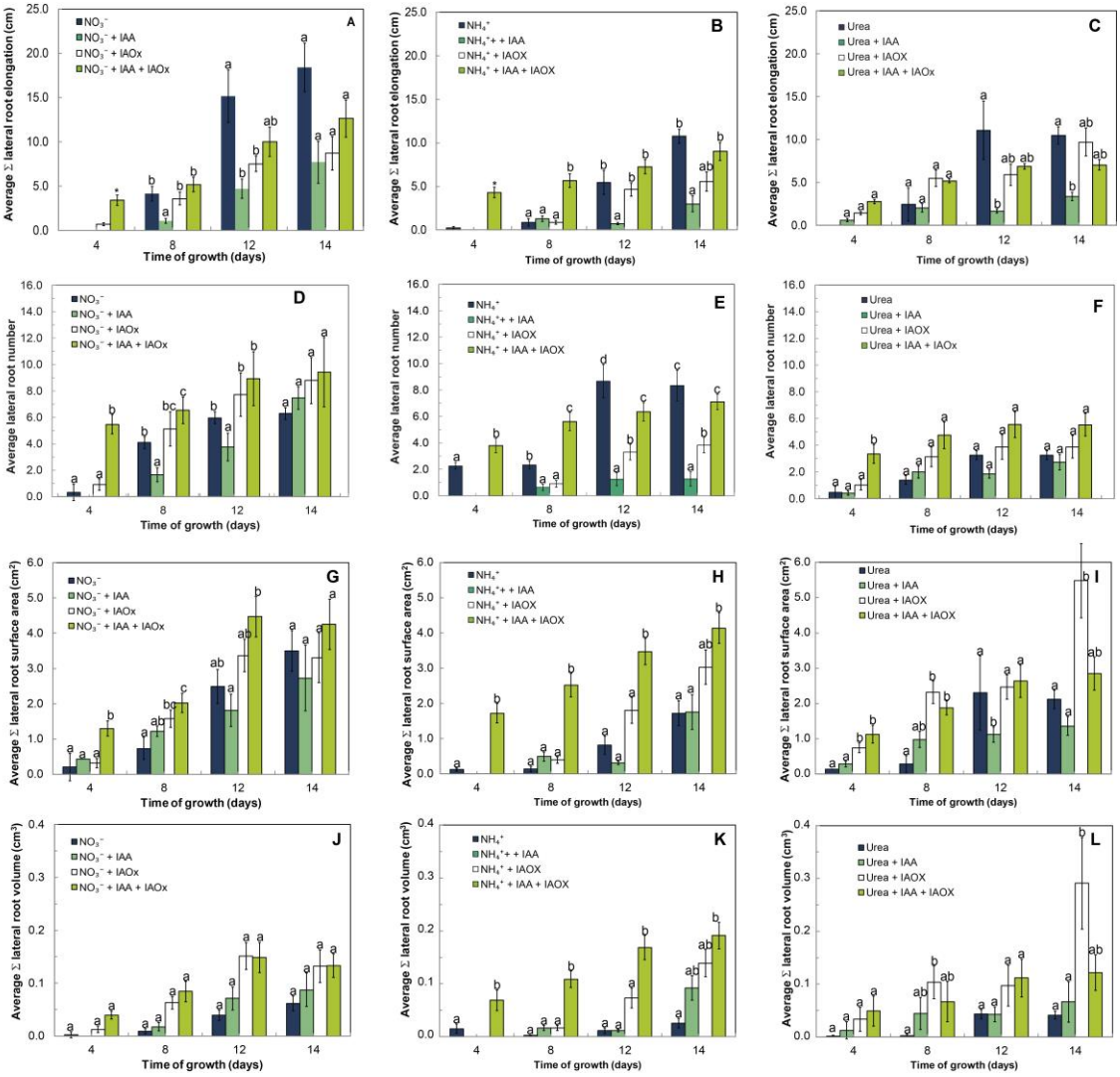

674

675 Fig. 4. Effect of IAOx, IAA and the combined effect of both on the lateral roots elongation
676 (cm), surface (cm^2) and volume (cm^3) of *M. truncatula* seedlings grown for 14 days under
677 1mM of NO_3^- (A, D, G, J), NH_4^+ (B, E, H, K) or urea (C, F, I, L). The values are the mean of
678 15-20 replicates ± S.E. An analysis of variance was performed considering the treatment as a
679 fixed factor. Asterisks in panels A, B and C indicate significant differences (α =0.05) between
680 treatments. In the rest of the panels different superscripted letters denote statistically significant
681 differences at α =0.05 using Student-Newman-Keuls tests.

682

683 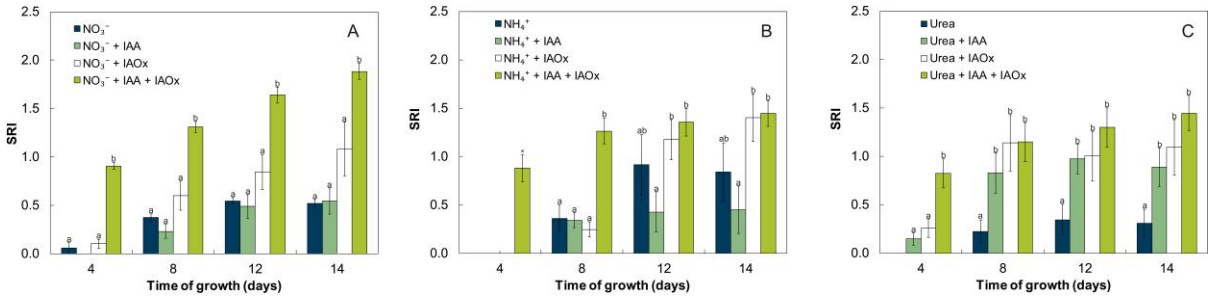

684 Fig. 5. Effect of IAOx, IAA and the combined effect of both on the "superroot index" (SRI) in
685 *M. truncatula* seedlings grown under NO_3^- (A), NH_4^+ (B) or urea (C). The values are the mean
686 of 15-20 replicates ± S.E. An analysis of variance was performed for the end of the experiment
687 considering the treatment as a fixed factor. Different superscripted letters denote statistically
688 significant differences at $\alpha = 0.05$ using Student-Newman-Keuls tests.

689

690 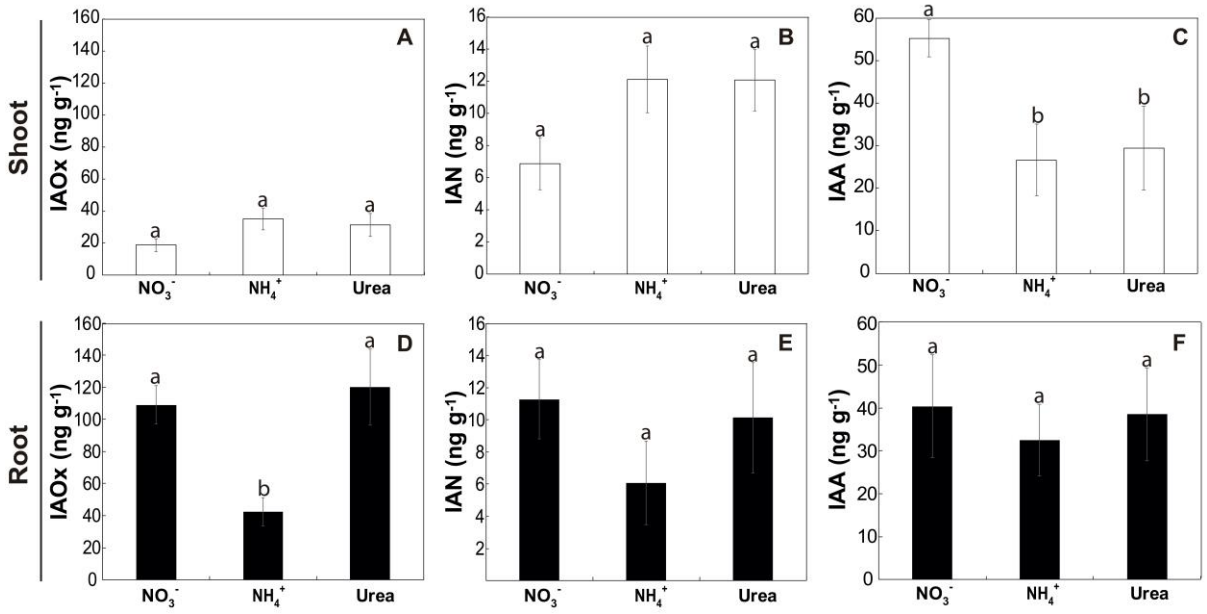

691 Fig. 6. IAOX (A, D), IAN (B, E) and IAA (C, F) contents (ng g FW^{-1}) in *M. truncatula*
692 seedlings grown under NO_3^-, NH_4^+ and urea. White and black bars indicate shoots and roots
693 respectively. The values are the means of 4-6 replicates ± S.E. Different superscripted letters
694 denote statistically significant differences at $\alpha = 0.05$ after Student–Newman–Keuls tests. No
695 superscripted letters in the bars indicate no statistically significant differences at $\alpha = 0.05$
696

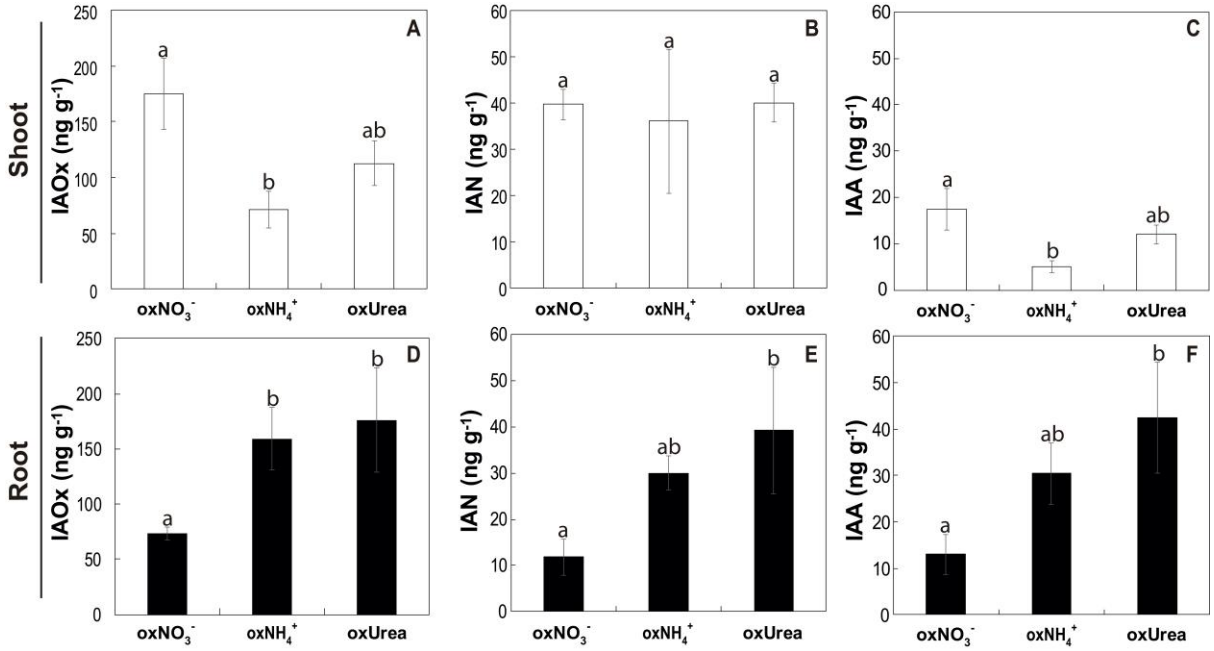

Fig. 7. IAOX (A, D), IAN (B, E) and IAA (C, F) contents (ng g FW^{-1}) in *M. truncatula* seedlings grown under NO_3^-, NH_4^+ and urea with 200µM of IAOX ($_{OX}NO_3^-$, $_{OX}NH_4^+$ and $_{OX}$urea). White and black bars indicate shoots and roots respectively. The values are the means of 4-6 replicates ± S.E. Different superscripted letters denote statistically significant differences at $\alpha = 0.05$ after Student–Newman–Keuls tests. No superscripted letters in the bars indicate no statistically significant differences at $\alpha = 0.05$

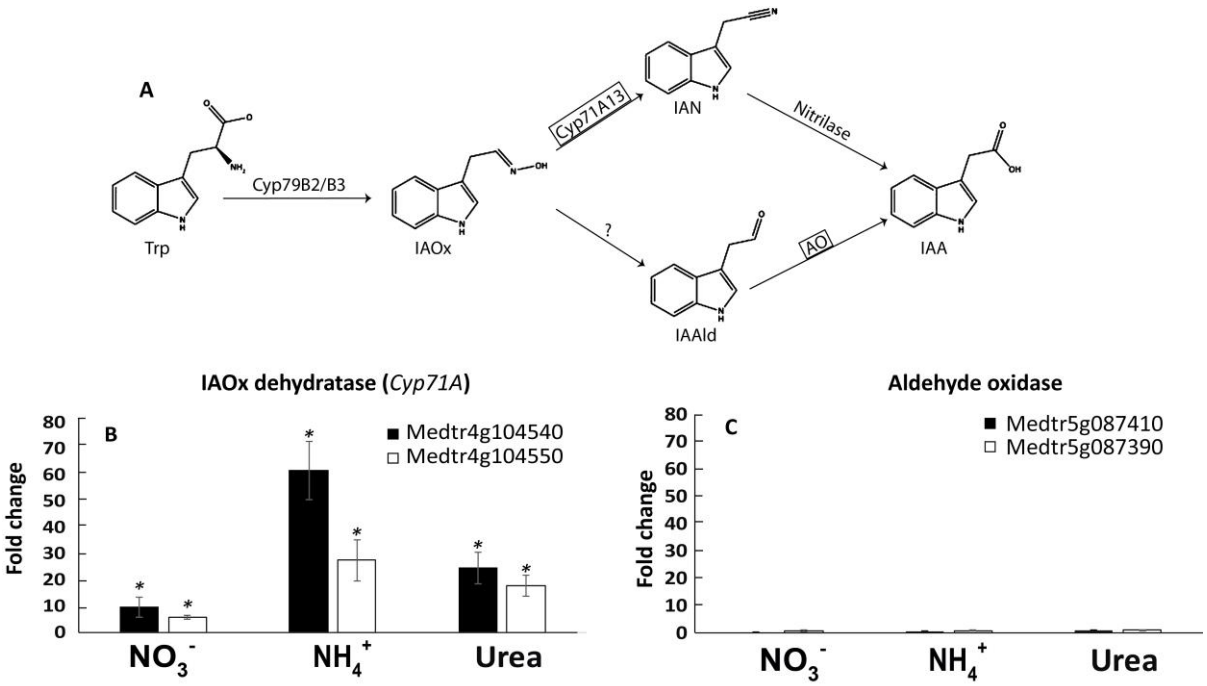

Fig. 8. Proposed Trp-dependent IAA synthesis route from IAOx in *Arabidopsis thaliana*, representing two of the possible synthesis pathways downstream of IAOx (Modified from ref. 7) (A). Transcript levels of *Medtr4g104540* and *Medtr4g104550* encoding for CYP71A members (B) and *Medtr5g087410*and *Medtr5g087390* encoding for aldehyde oxidases (C) expressed in fold change with respect to the control. * Denotes statistically significant differences relative to the non-treated control ($\alpha<0.05$).